

ORIGINAL RESEARCH



MERTK inhibition improves therapeutic efficacy of immune checkpoint inhibitors in hepatocellular carcinoma

Diana Llopiz^{a,b,c}, Leyre Silva^{a,b,c}, Marta Ruiz^{a,b,c}, Carla Castro-Alejos^{a,b,c}, Belen Aparicio^{a,b,c}, Lucia Vegas^a, Stefany Infante^{a,d,e}, Eva Santamaria^d, and Pablo Sarobe^{a,b,c} 

^aProgram of Immunology and Immunotherapy, Cima Universidad de Navarra, Cancer Center Clínica Universidad de Navarra (CCUN), Pamplona, Spain; ^bNavarra Institute for Health Research (IDISNA), Pamplona, Spain; ^cCIBERehd, Pamplona, Spain; ^dDNA and RNA Medicine Division, Center for Applied Medical Research (CIMA), University of Navarra, Pamplona, Spain; ^eFacultad de Medicina Humana, Universidad de Piura, Lima, Peru

ABSTRACT

Immunotherapy with immune checkpoint inhibitors (ICI) in hepatocellular carcinoma (HCC) patients only achieves response rates of 25%–30%, indicating the necessity of new therapies for non-responder patients. Since myeloid-related suppressive factors are associated with poor responses to ICI in a subgroup of HCC patients, modulation of these targets may improve response rates. Our aim was to characterize the expression of the efferocytosis receptor MERTK in HCC and to analyze its potential as a new therapeutic target. In HCC patients, MERTK was expressed by myeloid cells and was associated with poorer survival. In a murine HCC model with progressive myeloid cell infiltration, MERTK was detected in dendritic cells and macrophages with an activated phenotype, which overexpressed the checkpoint ligand PD-L1. Concomitant expression of PD-1 in tumor T-cells suggested the pertinence of combined PD-1/PD-L1 and MERTK blockade. In vivo experiments in mice showed that inhibition of MERTK improved the therapeutic effect promoted by anti-PD-1 or by ICI combinations currently approved for HCC. This effect was associated with enhanced tumor infiltration and superior activity of antigen presenting cells and effector lymphocytes. Our results indicate that MERTK may behave as a relevant target for immunotherapeutic combinations in those HCC patients with tumors enriched in a myeloid component.

ARTICLE HISTORY

Received 15 October 2024
Revised 29 January 2025
Accepted 24 February 2025

KEYWORDS

Hepatocellular carcinoma; immune checkpoint inhibitors; MERTK; tumor-associated macrophages; dendritic cells

Introduction



Patients with advanced hepatocellular carcinoma (HCC) are treated with immune checkpoint inhibitors (ICI) blocking PD-L1 + VEGF or PD-L1 + CTLA-4.^{1,2} Response rates reach a 25–30% and are common in patients with a tumor micro-environment (TME) enriched in lymphocytes. However, limited responses are observed in patients with a poor preexisting immunity and lack of expansion of effector lymphocytes upon therapy.³ Therefore, new strategies are necessary to increase response rates in patients lacking the appropriate TME, such as those containing an immune exhausted/suppressive TME.^{4,5} Here, blockade of additional immunosuppressive targets would be necessary to overcome ICI resistance.


Immunosuppressive myeloid cells, including myeloid-derived suppressor cells (MDSC),⁶ tolerogenic dendritic cells (DC)⁷ and tumor-associated macrophages (TAM),^{8,9} inhibit antitumor immunity in HCC. Targeting these cells and/or their associated inhibitory molecules would reinforce their antitumor properties and their cross-talk with effector T-cells.¹⁰ We previously demonstrated that vaccination upregulated the immunomodulatory molecule MERTK in DC, and its blockade improved vaccine potency, resulting in superior therapeutic effect, which was potentiated by combination with ICI.¹¹ MERTK, a member of the Tyro3/Axl/Mertk receptor

tyrosine kinase family, is involved in efferocytosis¹² and has immunomodulatory properties in DC and macrophages,¹³ inhibiting their TLR-dependent activation.¹⁴ Characterization of these immunomodulatory properties has prompted the development of strategies using MERTK inhibitors in cancer immunotherapy, in some cases in combination with ICI.¹⁵

Antitumor immunity in HCC is developed in the tolerogenic hepatic milieu and can be co-opted by the tumor micro-environment to escape from immune surveillance.¹⁶ HCC patients with increased MERTK expression had poorer overall survival and MERTK expression in HCC cells modulates its metabolism, proliferation and resistance to immunotherapy,^{17,18} pointing out to its relevance in HCC. However, these studies mainly considered the role of MERTK in tumor, but not myeloid cells, where it can modulate tumor immune control and escape, as well as the efficacy of immunotherapy.

Thus, we investigated MERTK expression in human and murine HCC, to understand its role and the potential effect that MERTK inhibition would have on tumor growth and response to immunotherapy. We show that in human and murine HCC, MERTK is mainly expressed in myeloid cells. In murine HCC MERTK is found in activated DC and macrophages that overexpress PD-L1. Combination of ICI with

CONTACT Pablo Sarobe  psarobe@unav.es  Program of Immunology and Immunotherapy, Cima Universidad de Navarra, Cancer Center Clínica Universidad de Navarra (CCUN), Pío XII 55, Pamplona 31008, Spain

 Supplemental data for this article can be accessed online at <https://doi.org/10.1080/2162402X.2025.2473165>

© 2025 The Author(s). Published with license by Taylor & Francis Group, LLC.

This is an Open Access article distributed under the terms of the Creative Commons Attribution-NonCommercial License (<http://creativecommons.org/licenses/by-nc/4.0/>), which permits unrestricted non-commercial use, distribution, and reproduction in any medium, provided the original work is properly cited. The terms on which this article has been published allow the posting of the Accepted Manuscript in a repository by the author(s) or with their consent.

MERTK inhibition results in improved therapeutic efficacy, indicating that MERTK could be a promising target for combinatorial immunotherapies in HCC patients with tumors enriched in myeloid cells.

Materials and methods

Analysis of MERTK expression in human samples and survival studies

MERTK expression in HCC samples was analyzed using TNMplot¹⁹ and TISCH2.²⁰ Survival studies were done using Kaplan-Meier Plotter²¹ and patients were stratified using the option which auto-selects the best cutoff percentile.

Mice

Female C57BL/6J mice (8 weeks old) were obtained from Envigo. MERTK KO mice (*Mertk*^{tm1Grl})²² were kindly obtained from Dr G. Lemke through Dr A. Morales and bred in our institution. They were maintained in pathogen-free conditions and treated according to the guidelines of our institutional Animal Research Ethics Committee (protocol 088–22).

Cell line

The HCC PM299L cell line, a kind gift of Dr A. Lujambio (MSSM, NY, USA), has been previously described.²³ It was obtained from a tumor generated in mice by hydrodynamic injection of plasmids MYC-lucOS (encoding MYC, luciferase and OVA peptides 257–264 and 323–339) and CTNNB1 (encoding a constitutive active beta-catenin form).

HCC tumor model and treatments

An orthotopic HCC tumor model was used, by inoculating intrahepatically 5×10^4 PM299L cells.²³ At different time points, tumors were obtained for analyses of the TME. For treatment, tumor size was evaluated by microCT at day 7 after inoculation, and mice with 4–5 mm diameter tumors were randomized: Antibodies (anti-PD-1 50 µg; anti-PD-L1 200 µg + anti-VEGFR 800 µg; anti-PD-L1 50 µg + anti-CTLA-4 50 µg; isotype control 50–800 µg, depending on the therapeutic antibody; all from Bioxcell) were administered i.p. at days 8, 11 and 14. The MERTK inhibitor RXDX-106 (Medchem) was administered orally (30 mg/kg) at days 8–17. At day 18 mice were sacrificed and tumors obtained. Volume was calculated with the formula $V = (D \times d^2)/2$, where D and d correspond to the large and small tumor diameters, respectively.

Flow cytometry

Tumors were digested with collagenase/DNase (Roche) for 15 min, homogenized and incubated with Fc BlockTM (BD-Biosciences) for 10 min. Then, they were stained with antibody panels (Supplementary Methods) to characterize myeloid and lymphoid cells. In cytokine secretion assays, after tumor homogenization, cells were stimulated for 4 h with PMA (0.05 µg/ml) and Ionomycin (0.5 µg/ml) in the

presence of GolgiStop/GolgiPlug (BD-Biosciences). After washing and surface staining, cells were treated with Cytofix/Cytoperm (BD-Biosciences) and stained with antibodies against IFN-γ and TNF-α. Dead cells were excluded with promofluor 840 (Maleimide). Next, cells were acquired with Cytoflex (Beckman Coulter) flow cytometer and analyzed with FlowJo software.

In vitro cultures of bone marrow-derived macrophages and dendritic cells

For macrophage cultures, bone marrow cells (10^6 cells/well) were cultured in 12-well plates with M-CSF (100 ng/ml) and polarized toward M1 or M2 cells as described.²⁴ DC was differentiated by culturing 10^6 cells in 24-well plates with GM-CSF (20 ng/ml). At day 6, they were treated with the STING agonist cGAMP (10 µg/ml; Invivogen) or IFN-γ (50 ng/ml; Peprotech).

RNAseq and gene expression analyses

RNAseq experiments and analyses of results were carried out using tumor extracts from C57BL/6J mice treated with different immunotherapies (Supplementary Methods).

Statistical analyses

Statistical analyses were performed using GraphPad Prism v10. Normality was checked with Shapiro – Wilk. T-tests, ANOVA, Pearson correlation and non-parametric tests were used. A $p < 0.05$ was taken to represent statistical significance.

Results

MERTK is expressed on macrophages in HCC

We first analyzed MERTK expression in human HCC and observed levels similar to normal liver ($p = 0.309$) (Supplementary Figure S1a). Moreover, they did not change along pathological stages (Supplementary Figure S1b). According to TISCH2,²⁰ MERTK was mainly expressed in monocytes/macrophages, with a marginal expression in other immune cell subsets and also in malignant cells (Figure 1(a)). Higher MERTK expression is associated with poor outcomes in HCC patients, mainly for those with stage III–IV.¹⁷ Of note, MERTK expression negatively associates with survival of patients with grade 3 tumors ($p = 0.0052$) (Figure 1(b)), whereas no differences were observed for grade 1 and 2 tumors (Supplementary Figure S1c).

Expression of MERTK ligands GAS6 and PROS1 was also analyzed, showing a diverse expression profile, including leukocytic and non-leukocytic cells (endothelial, fibroblast, epithelial and malignant cells) (Supplementary Figure S1d).

Growth of orthotopic PM299L tumors associates with increasing levels of myeloid cells expressing MERTK

Given the relevance of MERTK in human HCC and its predominant expression in myeloid cells, we analyzed these subsets in the murine HCC orthotopic PM299L model

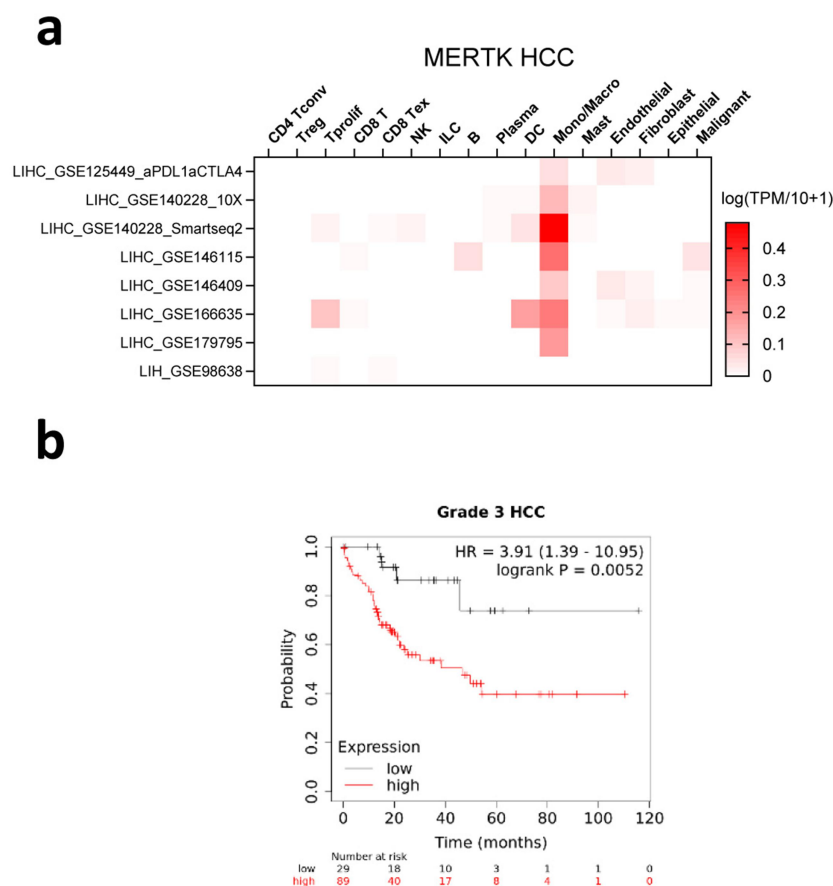


Figure 1. Expression of MERTK in human healthy and tumorous liver samples. (a) Expression of MERTK in HCC cell subsets according to TISCH2. (b) Overall survival of grade 3 HCC patients according to the expression of MERTK.

(Supplementary Figure S2). While the total leukocytic infiltrate (CD45⁺ cells) decreased with tumor growth, monocytes and monocyte-derived tumor-associated macrophages (TAM) increased. Remaining subsets (DC, Kupffer cells (KC) and MDSC) remained stable (Figure 2(a)). These changes were specific to tumor tissue, with lower levels of infiltrating leukocytes in tumors vs non-tumor regions or healthy liver (Figure 2(b)), and a general increase in myeloid cells in tumor tissue, with significant differences for TAM. Interestingly, lower proportions of KC were found in tumor tissue (Figure 2(b)).

Analyses of MERTK in leukocytes showed a predominant expression by myeloid cells, with DC and macrophages (TAM and KC) containing higher proportions of MERTK⁺ cells (16%, 13% and 16%, respectively) than monocytes and MDSC (<5%) (Figure 2(c)). Non-leukocytic CD45⁺ cells, mainly comprising tumor cells, showed a very low proportion (<1%) of MERTK⁺ cells (data not shown). To better understand the relevance of MERTK expressed by each of these myeloid cell subsets, we studied: (i) the relative contribution of each cell subset to the total pool of MERTK⁺ myeloid cells, observing that TAM and DC represented 62% and 20% of MERTK⁺ cells, compared with KC, monocytes and MDSC, with 7%, 5% and 3%, respectively (Figure 2(d)); (ii) the level of MERTK expression in these cells (measured as mean fluorescence intensity, MFI), with DC displaying the highest levels, followed by TAM and KC, whereas MDSC and monocytes had the lowest values (Figure 2(e)); and finally (iii) we defined the MERTK Score,

as the product of the percentage of MERTK⁺ cells in CD45⁺ cells and the MFI of MERTK in these cells. We observed that DC and TAM had the highest MERTK Score values, well above those found in remaining myeloid subsets (Figure 2(f)), indicating that DC and TAM are the most relevant populations in terms of MERTK expression.

Considering these features of MERTK expression, we analyzed a potential association between MERTK expressed by total myeloid cells, DC or TAM and tumor size, but no association was found in any case (Figure 2(g)).

MERTK⁺ myeloid cells have an activated phenotype

MERTK has been associated with immunoregulatory mechanisms.^{14,25} Accordingly, in a previous work, we demonstrated that MERTK inhibition during therapeutic vaccination enhanced vaccine efficacy.¹¹ In that context, in vitro use of the MERTK inhibitor RXDX-106²⁶ enhanced cytokine production and MHC-II expression by DC. To confirm the inhibitory role of MERTK in antigen presentation we cultured OVA-specific T cells with bone marrow-derived macrophages (BMDM) and OVA peptides, observing that in the presence of RXDX-106, a higher T cell proliferation was found (Supplementary Figure S3).

Thus, the phenotype of MERTK-expressing cell subsets was analyzed. MERTK⁺ TAM and DC contained higher proportions of CD86⁺ and PD-L1⁺ cells (Figure 3(a), upper panels). There was a positive correlation between MERTK expression levels

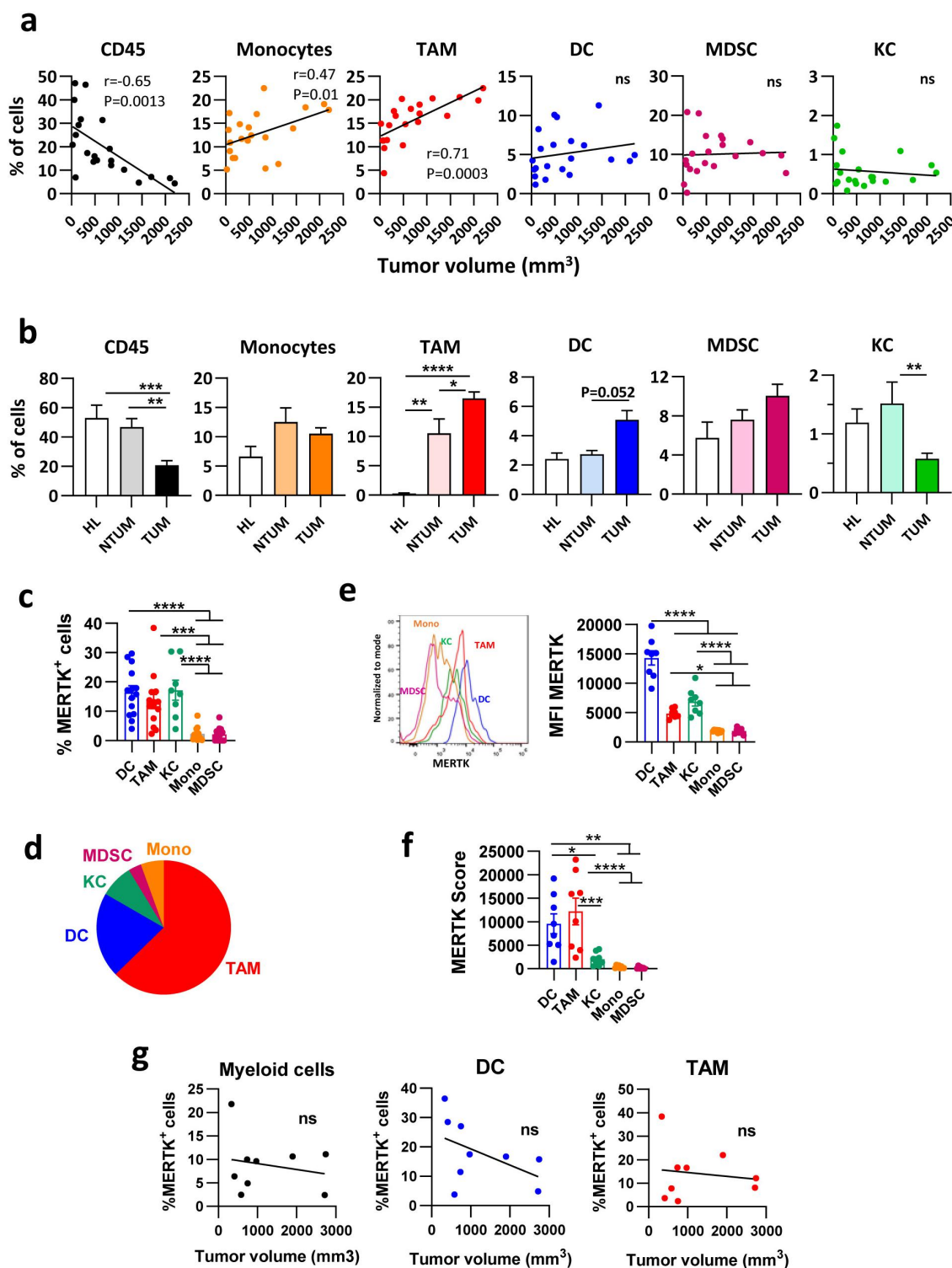


Figure 2. Evolution of myeloid cell subsets during murine PM299L HCC growth and expression of MERTK. (a) The presence of total leukocytes (among alive cells) and myeloid cells (in CD45⁺ cells) was analyzed by flow cytometry in PM299L HCC orthotopic tumors obtained at different time points. (b) Proportion of total leukocytes and myeloid cells in the liver of healthy mice (HL) ($n = 5$), and in tumor (TUM) ($n = 15$) and non-tumor (NTUM) ($n = 8$) samples. (c) Percentage of mertk-expressing cells in different myeloid subsets. (d) Contribution of each myeloid subset to total pool of MERTK⁺ cells. (e) Intensity of MERTK expression (measured as mean fluorescence index-MFI) in myeloid subsets. (f) MERTK score (product of the percentage of MERTK⁺ cells in CD45⁺ cells and the MFI of MERTK) of myeloid subsets. g. Correlation between tumor volume and the percentage of MERTK⁺ cells in total myeloid cells, DC and TAM (ns, non-statistically significant; * $p < 0.05$; ** $p < 0.01$; *** $p < 0.001$; **** $p < 0.0001$).

(measured as MFI) and MFI of CD86 and PD-L1 in TAM and DC (Figure 3(a), lower panels).

Given that CD86 has been considered an M1 marker in macrophages, we studied MERTK expression in TAM

according to their M1/M2 classification. By using CD38 and Arg1 as M1 and M2 markers, respectively, we found that most TAM corresponded to CD38⁺Arg1⁺ M2 subtype (Figure 3(b)), characterized by lower expression of CD86,

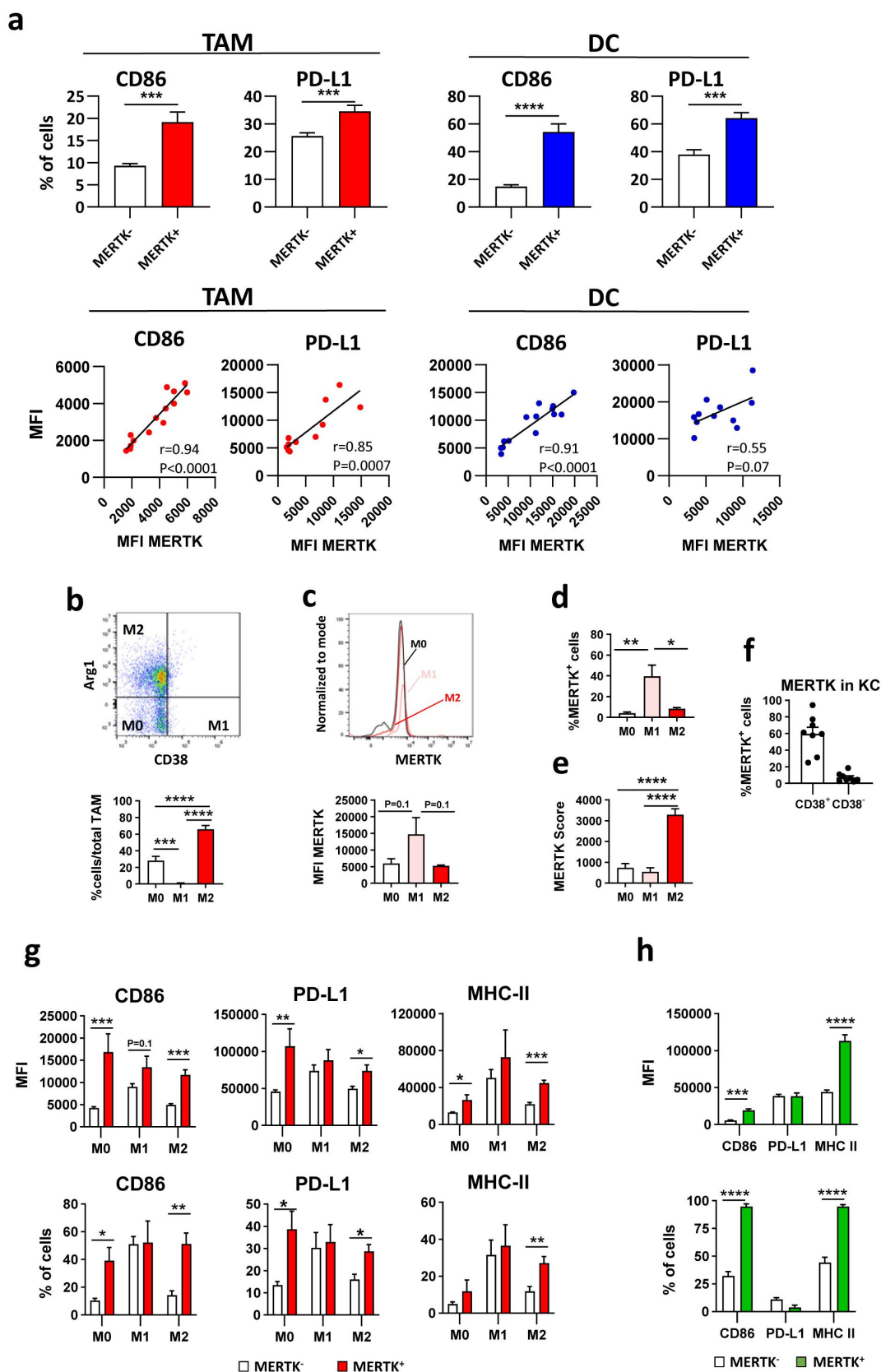


Figure 3. Phenotype of TAM and DC according to MERTK expression in orthotopic PM299L HCC tumors. (a) Percentage of TAM and DC expressing CD86 and PD-L1 according to MERTK expression ($n=6-12$ mice) (upper panels) and correlation of expression of these markers and MERTK, expressed as mean fluorescence intensity (MFI) (lower panels). (b) Identification of M0, M1 and M2 subsets within TAM. (c) Intensity of expression of MERTK (represented as MFI) in M0, M1 and M2 TAM. (d) Percentage of MERTK⁺ cells in M0, M1 and M2 TAM. (e) MERTK score of M0, M1 and M2 TAM. (f) Percentage of MERTK⁺ cells in KC according to CD38 expression. (g, h) MFI of CD86, PD-L1 and MHC-II (upper panels) and percentage of cells positive for these markers (bottom panels) in TAM (g) and in KC (h) was determined in MERTK⁺ and MERTK⁻ cells. (* $p < 0.05$; ** $p < 0.01$; *** $p < 0.001$; **** $p < 0.0001$).

PD-L1 and MHC-II than M1 TAM (Supplementary Figure S4).

Although MERTK has been described as a molecule mainly associated with M2 macrophages,²⁷ the few M1 TAM tended to express higher MERTK levels (MFI of MERTK) (Figure 3(c)) and contained a higher proportion of MERTK⁺ cells (Figure 3(d)). However, when we distributed the total MERTK Score corresponding to TAM between M0, M1 and M2 cells, M2 TAM had significantly superior values, presumably due to the higher presence of these cells (Figure 3(e)). Separate analysis of MERTK expression in KC showed that, as occurred with TAM, CD38⁺ KC contained a higher proportion of MERTK⁺ cells (Figure 3(f)).

Phenotypic characterization of these cells according to their MERTK expression showed that in M0 and M2 TAM, MERTK⁺ cells displayed higher levels of CD86, PD-L1 and MHC-II molecules than MERTK⁻ cells, whereas no differences were seen for M1 TAM (Figure 3(g), upper panels). Equivalent results were obtained when studying the proportions of cells positive for these markers (Figure 3(g), lower panels). These results were not restricted exclusively to monocyte-derived TAM, since those KC expressing MERTK had also higher levels of CD86 and MHC-II (Figure 3(h)). Overall, these results indicate that MERTK⁺ cells express higher levels of activation molecules.

We also studied the phenotype of in vitro polarized bone marrow-derived macrophages (BMDM) (Supplementary Figure S5a) and of bone marrow-derived DC (BMDC) according to MERTK expression. M1 macrophages had the highest expression of MERTK and high levels of CD86, PD-L1 and MHC-II (Supplementary Figure S5b). Similarly, cGAMP- and IFN- γ -activated BMDC had higher MERTK, CD86, PD-L1 and MHC-II expression than immature BMDC (Supplementary Figure S5c). Efferocytosis assays carried out using M0, M1 and M2 BMDM and apoptotic PM299L tumor cells showed that M1 macrophages had a higher efferocytic capacity (Supplementary Figure S5d), with higher proportions of CFSE^{hi} cells than M0 and M2 (21.7%, 30.6% and 19.8% for M0, M1 and M2, respectively). Finally, within M0, M1 and M2 macrophages (Supplementary Figure S5e), and in BMDC (Supplementary Figure S5f), MERTK⁺ cells usually had higher levels of CD80, CD86, PD-L1 and MHC-II and included higher percentages of cells expressing those markers, confirming in vitro the in vivo data associating MERTK expression with the presence of activation molecules.

MERTK correlates with higher levels of antigen experienced T-cells and promotes PD-L1 expression

Tumor-derived signals (with cGAMP as a surrogate) and T-cell-derived signals (IFN- γ), upregulated expression of MERTK and of other immunomodulatory molecules in DC and TAM, potentially affecting their cross-talk with lymphocytes. We thus analyzed the association between MERTK expression and lymphocyte presence (gating strategy in Supplementary Figure S6). In addition to total CD4 and CD8 T-cells, since PM299L cells express OVA peptides, we also analyzed OVA-specific CD8 T-cells (as a surrogate of tumor-specific T cells) by using MHC/OVA tetramers (TetOVA⁺

cells). Levels of total CD3 cells, CD4 T-cells and TetOVA⁺ CD8 T-cells decreased in larger tumors. No changes were found for total CD8 T-cells, Tregs, NK cells or B cells (Figure 4(a) and Supplementary Figure S7a). Tumor tissue contained increased levels of TetOVA⁺ CD8 T-cells and NK cells (Supplementary Figure S7b). Remarkably, tumor infiltrating CD8, CD4 and TetOVA⁺ T-cells contained a higher proportion of cells expressing PD-1, TIM-3 and LAG-3 (Supplementary Figure S7c). Of note, MERTK expression in total myeloid cells showed a trend for positive correlation with total leukocytes ($p = 0.058$), with a statistical significance for CD4 T-cells and TetOVA⁺ CD8 T-cells (Figure 4(b)). Moreover, whereas CD4 and TetOVA⁺ CD8 T-cells had a significant positive correlation with MERTK⁺ DC ($p = 0.0073$ and $p = 0.0091$, respectively), correlation was marginal with MERTK⁺ TAM ($p = 0.14$ and $p = 0.10$, respectively) (Supplementary Figure S8), suggesting a more relevant interaction of T cells with DC than with TAM. Finally, MERTK expression also correlated with levels of antigen-experienced T-cells (PD-1⁺ cells) (Figure 4(b)). Interestingly, many of these PD-1⁺ T-cells retained their functional capacity, since tumor T-cell stimulation with PMA/Ionomycin showed that PD-1⁺ T-cells produced IFN- γ , TNF- α or both cytokines, which in the case of CD8 T cells was higher than that observed for PD-1⁻ cells (Figure 4(c)). However, functionality of these tumor T-cells was lost with tumor growth, with lower cytokine levels produced by T-cells infiltrating large (>1000 mm³) tumors (Figure 4(d)).

Ligation of MERTK by Gas6/phosphatidylserine in tumor cells upregulates PD-L1 expression.²⁸ Moreover, MERTK inhibition decreases PD-L1 and PD-L2 expression in macrophages in a murine leukemia model.²⁹ Thus, we studied the effect of MERTK modulation on PD-L1 levels. Analyses of PD-L1 in hepatic myeloid cells showed that, although no differences were observed between hepatic macrophages in wild-type (WT) and MERTK KO mice, higher proportions of PD-L1⁺ DC were found in WT mice, with higher per cell levels (MFI) of PD-L1 (Figure 4(e)).

Therefore, PM299L tumor growth is associated with increasing levels of a myeloid infiltrate expressing MERTK and PD-L1, as well as with the presence of PD-1⁺ infiltrating lymphocytes, suggesting that MERTK and PD-1/PD-L1-dependent pathways could be targeted to enhance antitumor activity.

Simultaneous blockade of MERTK and PD-1 results in enhanced therapeutic efficacy

The role of MERTK in PM299L tumor growth was checked by using MERTK KO mice.²² The strain used, as opposed to other MERTK KO models, is known to have an improved anti-tumor immune response,³⁰ and according to it, a trend for smaller tumor volumes was observed in MERTK KO mice 18 days after tumor inoculation ($p = 0.09$). This was associated with a higher leukocytic infiltrate ($p = 0.12$) (Supplementary Figure S9a), suggesting that monotherapies based on MERTK inhibition would have a poor effect in tumor growth in our HCC model. PD-1 blockade in WT and MERTK KO mice did not decrease tumor size in any of the strains ($p = 0.24$ in WT mice

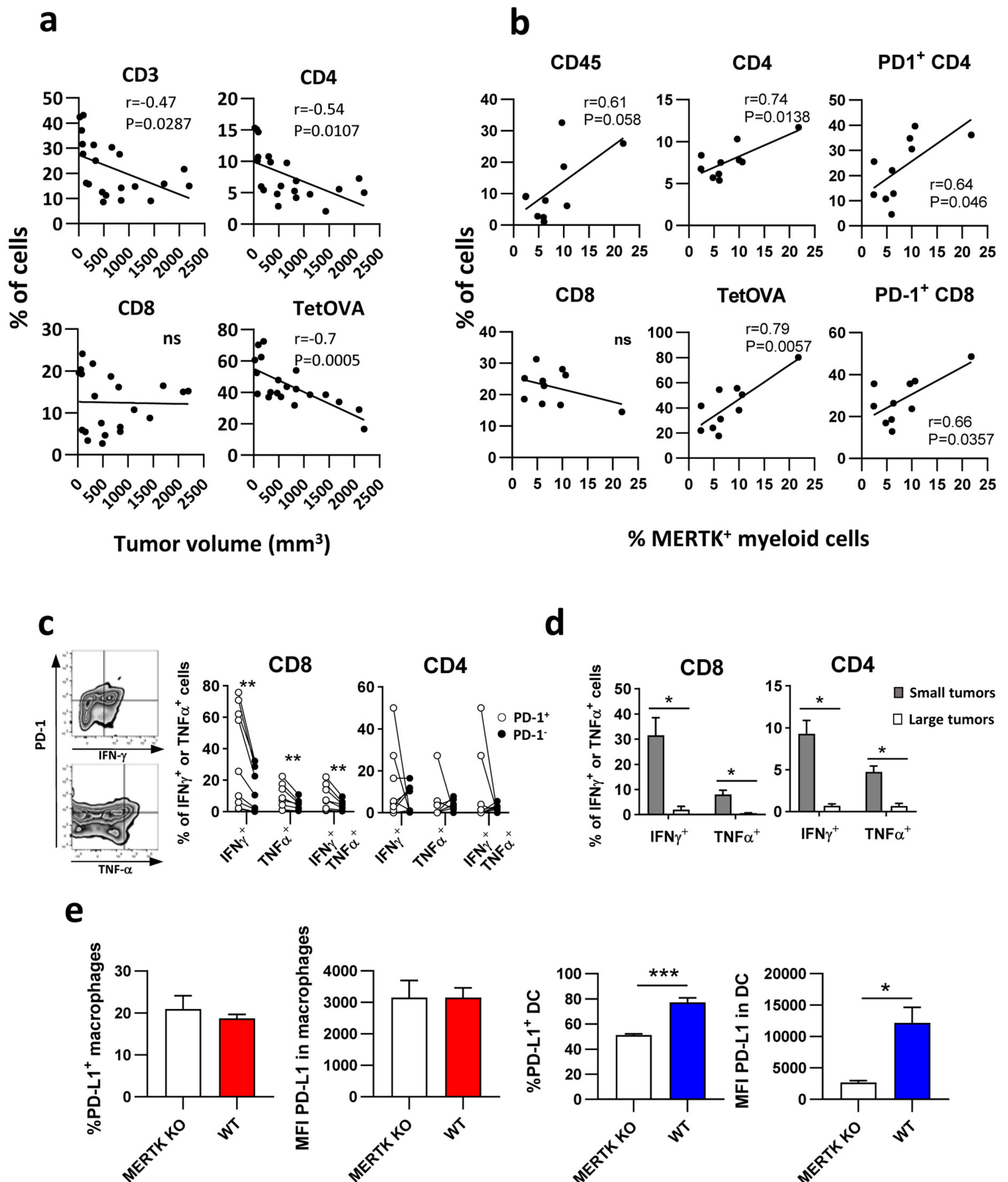


Figure 4. MERTK correlates with higher levels of antigen experienced T-cells and promotes PD-L1 expression. (a) The presence of lymphoid cells (in CD45⁺ cells) was analyzed in orthotopic PM299L HCC at different time points. (b) Correlation between percentage of CD45, CD4, CD8 and TetOVA⁺ cells, and of PD-1⁺ CD4 and PD-1⁺ CD8 cells, and the percentage of MERTK⁺ myeloid cells. (c) Tumor-infiltrating lymphocytes were stimulated with PMA/Ionomycin and cytokine production by PD-1⁺ and PD-1⁻ CD8 and CD4 T cells was determined by flow cytometry. (d) Production of cytokines after PMA/Ionomycin by CD8 and CD4 T cells obtained from small and large tumors. (e) PD-L1 expression was analyzed in hepatic macrophages (left panels) and DC (right panels) of wild type (WT) C57BL/6J and MERTK KO mice ($n = 5/\text{group}$). (* $p < 0.05$; ** $p < 0.01$; *** $p < 0.001$).

and $p = 0.76$ in MERTK KO mice). Again, MERTK KO mice treated with control antibodies had a trend for smaller tumor size when compared with WT mice ($p = 0.051$). Interestingly, MERTK KO mice treated with anti-PD-1 had significantly smaller tumors than WT mice treated with isotype control antibodies (Supplementary Figure S9b), suggesting that simultaneous blockade of PD-1 and MERTK would have a superior effect than monotherapies.

With these results, pharmacological inhibition of PD-1 and MERTK was tested by using anti-PD-1 antibodies and the MERTK inhibitor RXDX-106.²⁶ Anti-PD-1 alone had a negligible effect on tumor growth, as occurred with RXDX-106, in agreement with previous results using MERTK KO mice. However, their combination induced a significant decrease in tumor volume and weight (Figure 5(a)). In vitro, RXDX-106 demonstrated no effect on PM299L cell proliferation below 15 μ M (Supplementary Figure S10), in agreement with its poor antiproliferative capacity,²⁶ suggesting a lack of direct effect of RXDX-106 on tumor cells.

RNAseq studies carried out using tumor samples from treated mice showed that, compared with isotype-treated mice, most upregulated genes corresponded to the combination group (434 genes), whereas lower numbers of downregulated genes were observed in the different comparisons (Figure 5(b)). The combination upregulated genes grouped in immune-related pathways such as PD-1 signaling, T-cell activation, chemokines, cytokines and cytokine receptors (Figure 5(c)), as demonstrated for representative genes (Figure 5(e)) and confirmed in Protein–protein Interaction enrichment analyses (Figure 5(d)) and transcriptional regulatory networks (Supplementary Figure S11). This transcriptomic profile depicted a scenario with increased leucocyte infiltration and antigen presentation, leading to a higher effector lymphocyte activation.

Flow cytometry confirmed increased levels of CD45⁺ and TetOVA⁺ cells. Regarding myeloid cells, the combination group contained higher proportions of PD-L1⁺ TAM, presumably due to the higher inflammatory microenvironment, and of CD38⁺ TAM, indicating a shift toward an M1 profile (Figure 5(f)). Thus, combined blockade of PD-1 and TAM receptors results in enhanced antitumor effect associated with improved immunity.

Combination of MERTK blockade with approved HCC immunotherapies improves their efficacy

We were interested in testing the effect of MERTK blockade in combination with currently approved immunotherapies for HCC.^{1,2} Combination of RXDX-106 with anti-PD-L1 + anti-VEGFR (murine VEGF-blocking antibodies were not available) led to the highest tumor volume reduction (Figure 6(a)). When using anti-PD-L1 + anti-CTLA-4, although this combination did not achieve statistically significant differences with isotype-treated mice, addition of RXDX-106 led to significantly smaller tumors (Figure 6(b)). Flow cytometry analyses showed that MERTK blockade increased CD45⁺ cell levels, mainly associated with CD4 T-cells. Regarding myeloid cells, reduced proportions of DC were observed after combining RXDX-106 with any of the immunotherapies, whereas

a decrease on MDSC and TAM was found when combining RXDX-106 with anti-PD-L1 + anti-VEGFR or with anti-PD-L1 + anti-CTLA-4, respectively (Figure 6(c–d)).

RNAseq analyses performed using tumor samples obtained after treatment with anti-PD-L1 + anti-CTLA-4 \pm RXDX-106 showed that, as compared with isotype-treated mice, immunotherapy and the combination containing RXDX-106 upregulated 600 and 840 genes, respectively, whereas 205 and 259 genes were downregulated in these groups (Figure 6(e)). Since only 21 genes were differentially expressed between immunotherapy and the combination, we analyzed their differences with respect control mice. Upregulated genes enriched only in the combination group corresponded to activation of myeloid subsets (myeloid DC activation, antigen processing and presentation via MHC-II, positive regulation of macrophage fusion) and to T-cell response-associated pathways (positive regulation of Th1 cytokine production) (Figure 6(f)). Genes commonly upregulated by immunotherapy and by the combination were associated with pathways involved in positive regulation of immune activation, such as inflammasome, inflammatory responses or Fc gamma receptor signaling, among others (Supplementary Figure S12a). No immune-related pathways were found among genes exclusively enriched in mice treated with immunotherapy (Supplementary Figure S12b) or in down-regulated genes in any of the groups (Supplementary Figure S12c). Thus, combination of RXDX-106 with currently approved immunotherapies enhances its therapeutic efficacy, related to a higher leukocyte infiltration that involves more active lymphoid and myeloid compartments.

Discussion

Immunosuppressive myeloid cells may inhibit response to immunotherapy in HCC patients.^{31–33} Modulation of these cells would help to reinforce their antitumor activity while improving their cross-talk with effector lymphocytes, favoring immunotherapy response. We focused on MERTK, efferocytic receptor that downregulates myeloid cell activity.¹⁴ Although previous works have reported MERTK expression in tumor cells as a resistance mechanism to checkpoint inhibitors,¹⁸ patient analyses indicated a higher expression in myeloid cells (macrophages and DC). Interestingly, MERTK expression has a higher impact on survival in patients with less differentiated and more aggressive tumors, probably related to the relevance that macrophages acquire in this setting.⁵ However, we cannot discard that the association between MERTK expression and survival could be associated with higher macrophage infiltration in these patients. Our murine HCC model mirrors human findings, demonstrating preferential expression in TAM and DC, associated with progressive recruitment of monocyte-derived TAM as tumor grows. Previous reports associate MERTK expression with M2 macrophages.²⁷ Our in vivo and in vitro data reveal MERTK expression in all TAM subsets. However, despite higher MERTK levels in M1 TAM, M2 TAM had the highest contribution to MERTK expression in TAM (MERTK Score), confirming the relevance of M2 macrophages in MERTK expression.

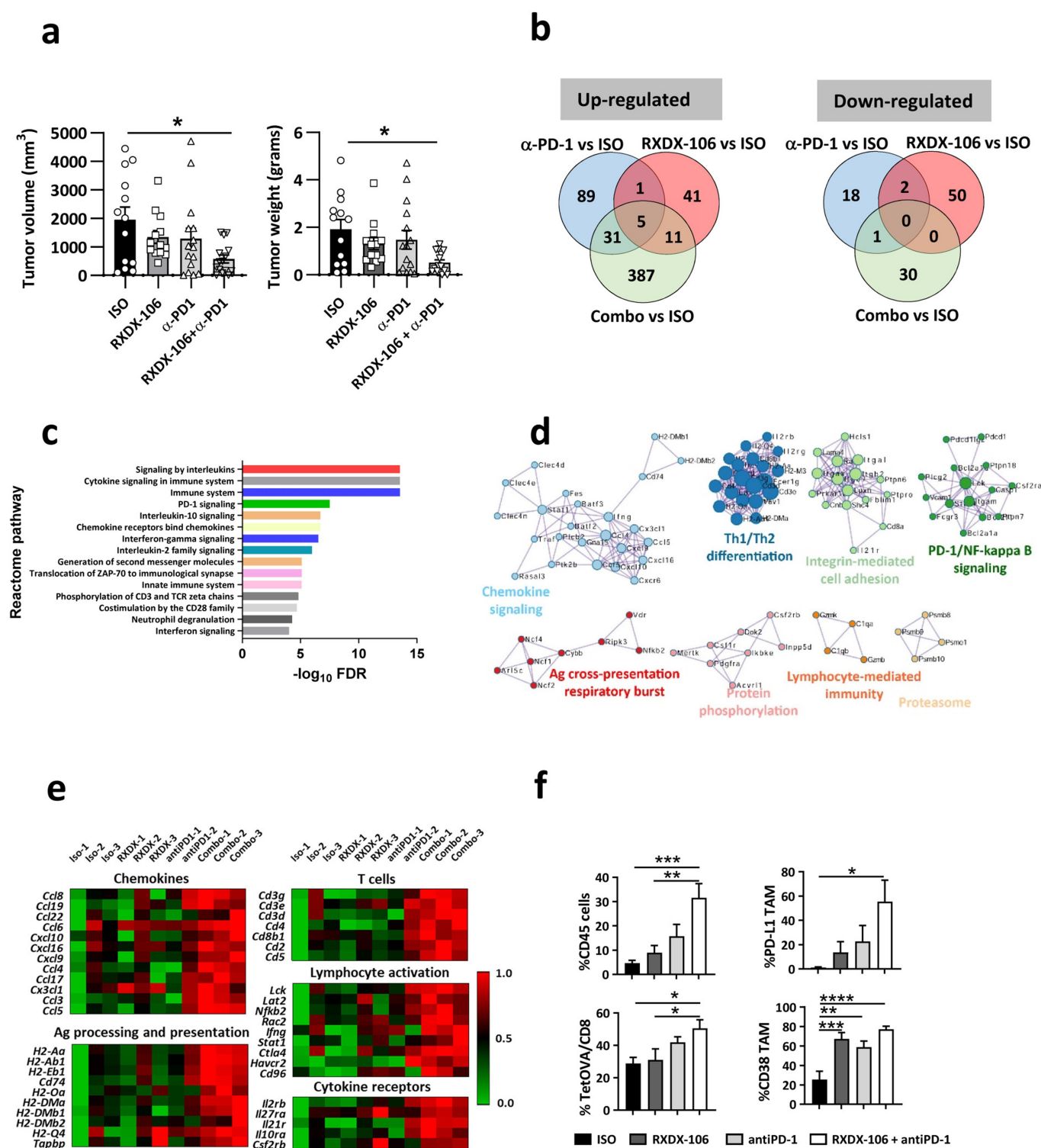


Figure 5. Simultaneous blockade of MERTK and PD-1 results in enhanced therapeutic efficacy. (a) C57BL/6J mice with orthotopic PM299L tumors were treated with control (ISO) or anti-PD-1 antibodies, RXDX-106, or the combination (RXDX-106 + anti-PD-1). They were sacrificed at day 18 to determine tumor volume and weight. (b) Number of up- and down-regulated genes in RNAseq experiments comparing tumor samples from isotype-treated mice (ISO) and treatment groups. (c) Pathway enrichment analyses according to reactome of genes upregulated by the combination vs ISO. (d) Protein-protein interaction networks of genes upregulated by the combination vs ISO according to Metascape. (e) Normalized expression of individual genes corresponding to immune functions and cell components in the four groups. (f) Analysis by flow cytometry of tumor infiltrating cells of mice ($n = 7-9/\text{group}$) corresponding to the different treatments. (* $p < 0.05$; ** $p < 0.01$; *** $p < 0.001$; **** $p < 0.0001$).

In general, expression of MERTK in macrophages and DC was associated with increased levels of MHC, co-stimulatory and co-inhibitory molecules. This was observed in vivo and in vitro, after activation with the STING agonist cGAMP (as

a tumor surrogate) or with the T-cell derived stimulus IFN- α . This would suggest that, as for other immunosuppressive molecules (e.g. PD-L1, IDO),³⁴ MERTK may be upregulated as a negative feedback mechanism to counteract

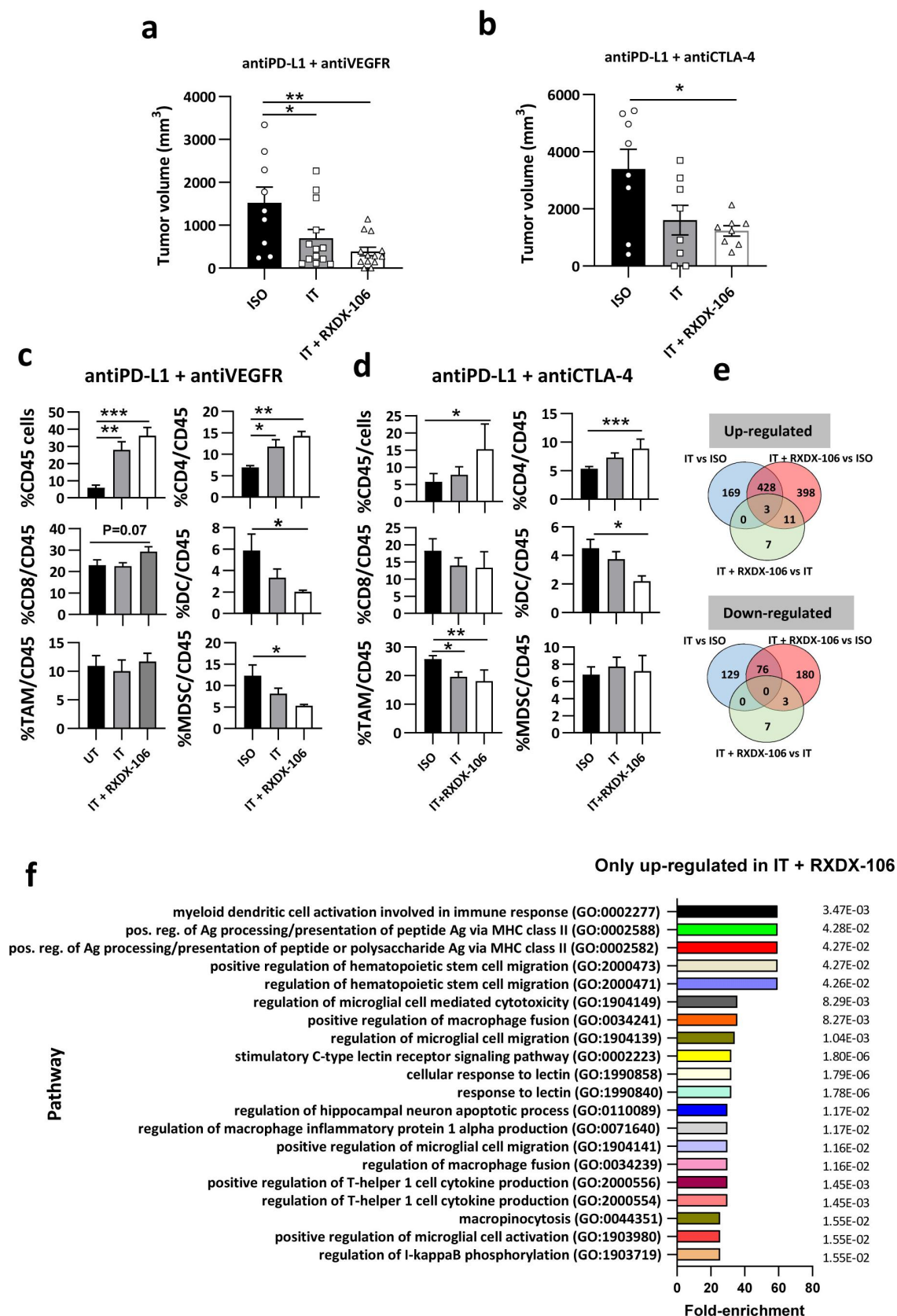


Figure 6. Combination of MERTK blockade with approved HCC immunotherapies improves their efficacy. C57BL/6J mice with orthotopic PM299L tumors were treated with control (ISO), immunotherapy (IT) based on blockade of PD-L1 + VEGFR (a), IT based on blockade of PD-L1 + CTLA-4 (b), or combination of these IT with RXDX-106, and tumor volume was determined. Flow cytometry analyses of tumor infiltrating cells obtained from mice ($n = 5-8$ mice/group) treated with PD-L1 + VEGFR (c) or PD-L1 + CTLA-4 (d) IT combinations. (e) Genes up- and down-regulated in mice treated with ISO, PD-L1 + CTLA-4 blockade (IT) or IT + RXDX-106 in RNAseq experiments using tumor samples ($n = 4$ mice/group) from each groups. (f) Pathway enrichment analyses of genes upregulated only by IT + RXDX-106.

inflammatory signals. Accordingly, infiltrating CD4 T-cells and tumor-specific (TetOVA⁺) CD8 T-cells, including PD-1-expressing CD4 and CD8 T-cells, positively correlated with MERTK expression. The stronger correlation of infiltrating CD4 and TetOVA⁺ T-cells with MERTK⁺ DC than with MERTK⁺ TAM might indicate that T-cell-derived signals would have a higher impact on MERTK expressed by DC, whereas MERTK expression on TAM would depend more on other signals. Indeed, most MERTK expression on TAM occurs in M2 cells, which as opposed to the small presence of M1, would not depend on inflammatory cytokines. Changes in the proportion of functional T-cells, DC and TAM during tumor growth may lead to different levels of MERTK expression by the myeloid cell subsets, resulting in a compensatory effect that maintains overall MERTK expression without significant changes.

In myeloid cells, besides inhibiting TLR-derived signals,¹⁴ MERTK may upregulate other immunosuppressive pathways, such as PD-L1, as reported in tumor cells. Our data using MERTK KO mice indicate that in the absence of MERTK signaling, lower PD-L1 expression is observed, in agreement with data obtained in a murine leukemia model.²⁹ Altogether, the association of myeloid MERTK with enhanced PD-L1 levels, and the presence of tumor-infiltrating PD-1⁺ T-cells, suggest that combined inhibition of MERTK and PD-1/PD-L1 would have a better therapeutic effect.

In our model, combining MERTK blockade with anti-PD-1 had a superior efficacy than monotherapies. In other murine tumors, RXDX-106 alone has demonstrated antitumor effects,²⁶ as well as when combined with a vaccine,¹¹ suggesting a higher activity in lymphocyte infiltrated tumors. In our myeloid-enriched HCC model, mechanisms responsible for the efficacy of the combination involve targeting myeloid cells, by increasing antigen processing and presentation machinery (as demonstrated in vitro), and lymphoid cells, promoting their infiltration and activation, which may also contribute to the superior lymphocytic activity.

Although initial HCC immunotherapy trials targeted PD-1,¹⁶ currently approved therapies contain ICI combinations.^{1,2} MERTK blockade with these regimes also resulted in superior in vivo efficacy, associated again with higher lymphocytic infiltrate, but with different effects on the myeloid compartment, depending on the combination. VEGF blockade inhibits immunosuppressive pathways that operate in myeloid cells,³⁵ while CTLA-4 inhibition is supposed to act mainly on T-cells.³⁶ Gene expression analyses of MERTK + PD-L1/CTLA-4 blockade demonstrated activation of myeloid subsets and T-cell response-associated pathways (Th1 cytokine production), highlighting the relevance of simultaneous targeting the myeloid and lymphoid compartments in these tumors enriched in immunosuppressive myeloid cells.

In summary, our data indicate that MERTK blockade may improve therapeutic efficacy of ICI in myeloid-enriched HCC tumors, opening the way for new therapies in HCC patients.

Acknowledgments

Authors thank Dr A. Lujambio for providing PM299L tumor cell line, Dr G. Lemke and Dr A. Morales for MERTK KO mice and M. Gorraiz for her help with proliferation assays.

Disclosure statement

No potential conflict of interest was reported by the author(s).

Funding

This work was supported by Gobierno de Navarra [grant GNS-54-2021] and Instituto de Salud Carlos III co-financed by European Union [grant PI23/00190].

ORCID

Pablo Sarobe  <http://orcid.org/0000-0003-0503-7905>

Data availability statement

The data supporting this study are available from the corresponding author upon reasonable request.

Abbreviations

ICI	immune checkpoint inhibitors
HCC	hepatocellular carcinoma
DC	dendritic cells
MDSC	myeloid-derived suppressor cells
TAM	tumor-associated macrophages
KC	Kupffer cells
BMDM	bone marrow-derived macrophages
BMDc	bone marrow-derived DC

References

1. Finn RS, Qin S, Ikeda M, Galle PR, Ducreux M, Kim TY, Kudo M, Breder V, Merle P, Kaseb AO, et al. Atezolizumab plus bevacizumab in unresectable hepatocellular carcinoma. *N Engl J Med*. 2020;382(20):1894–1905. doi:10.1056/NEJMoa1915745.
2. Abou-Alfa GK, Lau G, Kudo M, Chan SL, Kelley RK, Furuse J, Sukeepaisarnjaroen W, Kang Y-K, Van Dao T, De Toni EN, et al. Tremelimumab plus durvalumab in unresectable hepatocellular carcinoma. *NEJM Evid*. 2022;1(8):1–12. doi:10.1056/evidoa2100070.
3. Zhu AX, Abbas AR, de Galarreta MR, Guan Y, Lu S, Koeppen H, Zhang W, Hsu CH, He AR, Ryoo BY, et al. Molecular correlates of clinical response and resistance to atezolizumab in combination with bevacizumab in advanced hepatocellular carcinoma. *Nat Med*. 2022;28(8):1599–1611. doi:10.1038/s41591-022-01868-2.
4. Keskin DB, Anandappa AJ, Sun J, Tirosh I, Mathewson ND, Li S, Oliveira G, Giobbie-Hurder A, Felt K, Gjini E, et al. Neoantigen vaccine generates intratumoral T cell responses in phase Ib glioblastoma trial. *Nature*. 2019;565(7738):234–239. doi:10.1038/s41586-018-0792-9.
5. Zheng H, Peng X, Yang S, Li X, Huang M, Wei S, Zhang S, He G, Liu J, Fan Q, et al. Targeting tumor-associated macrophages in hepatocellular carcinoma: biology, strategy, and immunotherapy. *Cell Death Discov*. 2023;9(1). doi:10.1038/s41420-023-01356-7.
6. Hoechst B, Ormandy LA, Ballmaier M, Lehner F, Kruger C, Manns MP, Greten TF, Korangy F. A new population of myeloid-derived suppressor cells in hepatocellular carcinoma

- patients induces CD4(+)CD25(+)Foxp3(+) T cells. *Gastroenterology*. 2008;135(1):234–243. doi:10.1053/j.gastro.2008.03.020.
7. Han Y, Chen Z, Yang Y, Jiang Z, Gu Y, Liu Y, Lin C, Pan Z, Yu Y, Jiang M, et al. Human CD14+ CTLA-4+ regulatory dendritic cells suppress T-cell response by cytotoxic T-lymphocyte antigen-4-dependent IL-10 and indoleamine-2,3-dioxygenase production in hepatocellular carcinoma. *Hepatology*. 2014;59(2):567–579. doi:10.1002/hep.26694.
 8. Zhang Q, He Y, Luo N, Patel SJ, Han Y, Gao R, Modak M, Carotta S, Haslinger C, Kind D, et al. Landscape and dynamics of single immune cells in hepatocellular carcinoma. *Cell*. 2019;179(4):829–845.e20. doi:10.1016/j.cell.2019.10.003.
 9. Song G, Shi Y, Zhang M, Goswami S, Afridi S, Meng L, Ma J, Chen Y, Lin Y, Zhang J, et al. Global immune characterization of hbv/hcv-related hepatocellular carcinoma identifies macrophage and T-cell subsets associated with disease progression. *Cell Discov*. 2020;6(1). doi:10.1038/S41421-020-00214-5.
 10. Agirre-Lizaso A, Huici-Izagirre M, Urretabizkaia-Garmendia J, Rodrigues PM, Banales JM, Perugorria MJ. Targeting the heterogeneous tumour-associated macrophages in hepatocellular carcinoma. *Cancers (Basel)*. 2023;15(20):4977. doi:10.3390/CANCERS15204977.
 11. Llopiz D, Ruiz M, Silva L, Repáraz D, Aparicio B, Egea J, Lasarte JJ, Redin E, Calvo A, Angel M, et al. Inhibition of adjuvant-induced TAM receptors potentiates cancer vaccine immunogenicity and therapeutic efficacy. *Cancer Lett*. 2021;499:279–289. doi:10.1016/j.canlet.2020.11.022.
 12. Scott RS, McMahon EJ, Pop SM, Reap EA, Caricchio R, Cohen PL, Earp HS, Matsushima GK. Phagocytosis and clearance of apoptotic cells is mediated by MER. *Nature*. 2001;411(6834):207–211. doi:10.1038/35075603.
 13. Rothlin CV, Carrera-Silva EA, Bosurgi L, Ghosh S. TAM receptor signaling in immune homeostasis. *Annu Rev Immunol*. 2015;33(1):355–391. doi:10.1146/annurev-immunol-032414-112103.
 14. Rothlin CV, Ghosh S, Zuniga EI, Oldstone MB, Lemke G. TAM receptors are pleiotropic inhibitors of the innate immune response. *Cell*. 2007;131(6):1124–1136. doi:10.1016/j.cell.2007.10.034.
 15. Miao YR, Rankin EB, Giaccia AJ. Therapeutic targeting of the functionally elusive TAM receptor family. *Nat Rev Drug Discov*. 2024;23(3):201–217. doi:10.1038/S41573-023-00846-8.
 16. Sangro B, Sarobe P, Hervás-Stubbs S, Melero I. Advances in immunotherapy for hepatocellular carcinoma. *Nat Rev Gastroenterol Hepatol*. 2021;18(8):525–543. doi:10.1038/s41575-021-00438-0.
 17. Liu Y, Lan L, Li Y, Lu J, He L, Deng Y, Fei M, Lu JW, Shangguan F, Lu JP, et al. N-glycosylation stabilizes MerTK and promotes hepatocellular carcinoma tumor growth. *Redox Biol*. 2022;54:54. doi:10.1016/j.redox.2022.102366.
 18. Wang S, Zhu L, Li T, Lin X, Zheng Y, Xu D, Guo Y, Zhang Z, Fu Y, Wang H, et al. Disruption of MerTK increases the efficacy of checkpoint inhibitor by enhancing ferroptosis and immune response in hepatocellular carcinoma. *Cell Rep Med*. 2024;5(2):101415. doi:10.1016/j.xcrim.2024.101415.
 19. Bartha Á, Györfy B. TNMplot.com: a web tool for the comparison of gene expression in normal, tumor and metastatic tissues. *Int J Mol Sci*. 2021;22(5):1–12. doi:10.3390/IJMS22052622.
 20. Sun D, Wang J, Han Y, Dong X, Ge J, Zheng R, Shi X, Wang B, Li Z, Ren P, et al. TISCH: a comprehensive web resource enabling interactive single-cell transcriptome visualization of tumor microenvironment. *Nucleic Acids Res*. 2021;49(D1):D1420–D1430. doi:10.1093/NAR/GKAA1020.
 21. Menyhart O, Nagy Á, Györfy B. Determining consistent prognostic biomarkers of overall survival and vascular invasion in hepatocellular carcinoma. *R Soc Open Sci*. 2018;5(12):181006. doi:10.1098/RSOS.181006.
 22. Lu Q, Gore M, Zhang Q, Camenisch T, Boast S, Casagrande F, Lai C, Skinner MK, Klein R, Matsushima GK, et al. Tyro-3 family receptors are essential regulators of mammalian spermatogenesis. *Nature*. 1999;398(6729):723–728. doi:10.1038/19554.
 23. Silva L, Egea J, Villanueva L, Ruiz M, Llopiz D, Repáraz D, Aparicio B, Lasarte-Cia A, Lasarte JJ, de Galarreta MR, et al. Cold-inducible RNA binding protein as a vaccination platform to enhance immunotherapeutic responses against hepatocellular carcinoma. *Cancers (Basel)*. 2020;12(11):1–18. doi:10.3390/CANCERS12113397.
 24. Llopiz D, Ruiz M, Villanueva L, Iglesias T, Silva L, Egea J, Lasarte JJ, Pivette P, Trochon-Joseph V, Vasseur B, et al. Enhanced anti-tumor efficacy of checkpoint inhibitors in combination with the histone deacetylase inhibitor belinostat in a murine hepatocellular carcinoma model. *Cancer Immunol Immunother*. 2019;68(3):379–393. doi:10.1007/S00262-018-2283-0.
 25. Carrera Silva EA, Chan PY, Joannas L, Errasti AE, Gagliani N, Bosurgi L, Jabbour M, Perry A, Smith-Chakmakova F, Mucida D, et al. T cell-derived protein S engages TAM receptor signaling in dendritic cells to control the magnitude of the immune response. *Immunity*. 2013;39(1):160–170. doi:10.1016/j.immuni.2013.06.010.
 26. Yokoyama Y, Lew ED, Seelige R, Tindall EA, Walsh C, Fagan PC, Lee JY, Nevarez R, Oh J, Tucker KD, et al. Immuno-oncological efficacy of RXDX-106, a novel TAM (TYRO3, AXL, MER) family small-molecule kinase inhibitor. *Cancer Res*. 2019;79(8):1996–2008. doi:10.1158/0008-5472.CAN-18-2022.
 27. Zizzo G, Hilliard BA, Monestier M, Cohen PL. Efficient clearance of early apoptotic cells by human macrophages requires M2c polarization and MerTK induction. *J Immunol*. 2012;189(7):3508–3520. doi:10.4049/jimmunol.1200662.
 28. Kasikara C, Kumar S, Kimani S, Tsou WI, Geng K, Davra V, Sriram G, Devoe C, Nguyen KQN, Antes A, et al. Phosphatidylserine sensing by TAM receptors regulates AKT-dependent chemoresistance and PD-L1 expression. *Mol Cancer Res*. 2017;15(6):753–764. doi:10.1158/1541-7786.MCR-16-0350.
 29. Lee-Sherick AB, Jacobsen KM, Henry CJ, Huey MG, Parker RE, Page LS, Hill AA, Wang X, Frye SV, Shelton Earp H, et al. MERTK inhibition alters the PD-1 axis and promotes anti-leukemia immunity. *JCI Insight*. 2018;3(21). doi:10.1172/JCI.INSIGHT.97941.
 30. Akalu YT, Mercau ME, Ansems M, Hughes LD, Nevin J, Alberto EJ, Liu XN, He LZ, Alvarado D, Keler T, et al. Tissue-specific modifier alleles determine *Mertk* loss-of-function traits. *Elife*. 2022;11:11. doi:10.7554/ELIFE.80530.
 31. Liu Y, Xun Z, Ma K, Liang S, Li X, Zhou S, Sun L, Liu Y, Du Y, Guo X, et al. Identification of a tumour immune barrier in the HCC microenvironment that determines the efficacy of immunotherapy. *J Hepatol*. 2023;78(4):770–782. doi:10.1016/j.jhep.2023.01.011.
 32. Fan G, Xie T, Li L, Tang L, Han X, Shi Y. Single-cell and spatial analyses revealed the co-location of cancer stem cells and SPP1+ macrophage in hypoxic region that determines the poor prognosis in hepatocellular carcinoma. *NPJ Precis Oncol*. 2024;8(1). doi:10.1038/S41698-024-00564-3.
 33. Shen K-Y, Zhu Y, Xie S-Z, Qin L-X. Immunosuppressive tumor microenvironment and immunotherapy of hepatocellular carcinoma: current status and perspectives. *J Hematol Oncol*. 2024;17(1):25. doi:10.1186/S13045-024-01549-2.
 34. Spranger S, Spaapen RM, Zha Y, Williams J, Meng Y, Ha TT, Gajewski TF. Up-regulation of PD-L1, IDO, and T(regs) in the melanoma tumor microenvironment is driven by CD8(+) T cells. *Sci Transl Med*. 2013;5(200). doi:10.1126/SCITRANSLMED.3006504.
 35. Shigetake K, Datta M, Hato T, Kitahara S, Chen IX, Matsui A, Kikuchi H, Mamessier E, Aoki S, Ramjiawan RR, et al. Dual programmed death receptor-1 and vascular endothelial growth factor receptor-2 blockade promotes vascular normalization and enhances antitumor immune responses in hepatocellular carcinoma. *Hepatology*. 2020;71(4):1247–1261. doi:10.1002/hep.30889.
 36. Ribas A, Wolchok JD. Cancer immunotherapy using checkpoint blockade. *Science (80-)*. 2018;359(6382):1350–1355. doi:10.1126/science.aar4060.